

OBSERVER BASED SPEED CONTROL OF BLDC MOTOR WITHOUT POSITION SENSORS

Sabeel Irshad B^{#1} and Sudarshan Patil Kulkarni^{*2}

[#]M.Tech (Industrial Electronics), Department of ECE, S J College of Engineering, Mysore, Karnataka, India

^{*}Professor (Industrial Electronics), Department of ECE, S J College of Engineering, Mysore, Karnataka, India

Abstract— In this paper a new position sensorless drive is proposed for brushless DC (BLDC) motors. Most of the sensorless control methods like back-EMF detection method demonstrate high performance just at a high speed range as the back-EMF's magnitude depends on the rotor speed. Therefore the rotor position is to be estimated by an unknown input observer over a high speed range, a trapezoidal back-EMF is considered as an unknown input in the proposed method. The rotor position is detected by the estimation of line-to-line back-EMF in real time which is done by unknown input observer. This observer shows high performance at a low speed range as the rotor position and the rotor speed is calculated separately with no extra circuit or complex operation method. The proposed control design is simulated using Matlab/Simulink software.

Index Terms— BLDC motor, Full speed range, Sensorless control, Unknown input observer

I. INTRODUCTION

DC motors are getting replaced by Brushless DC (BLDC) motors in various applications such as automotive, aviation and household appliances. These applications need a very strong, high power density and efficient motor for operation. Household appliances are one of the main applications for BLDCs. Common household appliances which use electric motors consists of air conditioners, refrigerators, vacuum cleaners, washers and dryers. These appliances have relied on traditional electric motors like single phase AC motors including capacitor-start, capacitor-run motors, and universal motors. However, consumers now claim better performance, less acoustic noise and higher efficient motor for their appliances. Hence, BLDC have been introduced in order to accomplish these requirements.

Brushless DC motors (BLDC) are usually limited horsepower control motors that provide several advantages such as high efficiency, quiet operation, high reliability, compact form and little maintenance. However, there are disadvantages of the BLDC because of variable speed, and therefore flexible speed drives are used to overcome this. Brushless DC (BLDC) motors have the advantage of higher power density than other motors like induction motors because of having no copper losses on the rotor side and they do not require mechanical commutation system in

comparison with DC motors, which results in compact and robust structures. Owing to these features, BLDC motors have become more prominent in the applications where efficiency is a critical issue, or where spikes caused by mechanical commutation are not allowed. A BLDC motor needs an inverter and a rotor position sensor to achieve commutation process because it does not have brushes and commutators as in DC motors. However, the position sensor presents a lot of disadvantages from the viewpoints of drive's cost, machine size, reliability, and noise immunity. Therefore, many researchers went for sensorless drives that can control speed, position, and/or torque without shaft-mounted position sensors [1], [2] and [21].

Conventional sensorless control methods can be classified into four types. First, the open phase current sensing method [3] is a technique for detecting the conducting period of freewheeling diodes connected in anti-parallel with power transistors. It has the advantage that the control characteristic has high performance at low speeds and the synchronous process is simple. However, rotor position resolution conspicuously reduces at high speeds. In particular, for realization of this method, it has the defect that an additional isolated power needs to be supplied to a comparator for detecting the freewheeling current. Second method is detecting the third harmonic of back-EMF [4], [5] is the technique to remove all the fundamental and other polyphase components by doing a simple summation of three phase voltages. There is a reduced filtering requirement for the integration function performed on the signal, which has a frequency three times that of the fundamental signal. Ultimately, the filter has a much smaller capacity than the flux detection method using back-EMF; it is not affected by filtering delays and achieves high performance over a wide speed range. However, a neutral point that is not considered in the manufacturing process of the motor is required to measure phase voltages. Also, at a low speed range the third harmonics detection is difficult. Thirdly, the back-EMF integrating method [6], [7] is a technique applying the principle that integration from Zero Crossing Point (ZCP) to 30° is constant. There is the advantage that it is not necessary to measure an additional conversion point of the switching mode. Therefore, operation of the main processor decreases. This method does not synchronize the phase current with the back-EMF at the sensorless drive. Besides, the flux-weakening drive is impossible. Finally, the open phase

voltage sensing method [8] - [11] is a scheme estimating the rotor position indirectly by using the ZCP detection of open phase's terminal voltage. It is the most commonly used sensorless control method. However, this method has a deteriorated response at transient state and requires high operational speed enough to detect the ZCP of terminal voltages. To solve above problems, this paper proposes a new sensorless control method utilizing an unknown input observer. The unknown input observer has been widely researched [12] - [14] and [22] - [23], especially in the fault detection field [15] - [17] and [24]. However, this observer has not been adopted in sensorless BLDC motor control application.

Hence, this paper introduces a new sensorless control method integrating an unknown input observer that is independent of the rotor speed for a BLDC motor drive. Therefore, this paper proposes a highly useful new solution for a sensorless BLDC motor drive, which estimates a line-to-line back-EMF effectively.

II. MODELLING OF BLDC MOTOR

Fig. 1 shows the block diagram of the BLDC motor drive.

Equation (1) gives the voltage of the three phases assuming equal stator resistances for all the windings and constant self and mutual inductances [18]. In this equation, magnets, stainless steel restraining sleeves with high resistivity, and rotor-induced currents are neglected and no damper windings are modeled.

$$\begin{bmatrix} v_a \\ v_b \\ v_c \end{bmatrix} = \begin{bmatrix} R_s & 0 & 0 \\ 0 & R_s & 0 \\ 0 & 0 & R_s \end{bmatrix} \begin{bmatrix} i_a \\ i_b \\ i_c \end{bmatrix} + \begin{bmatrix} L_s - M & 0 & 0 \\ 0 & L_s - M & 0 \\ 0 & 0 & L_s - M \end{bmatrix} \frac{d}{dt} \begin{bmatrix} i_a \\ i_b \\ i_c \end{bmatrix} + \begin{bmatrix} e_a \\ e_b \\ e_c \end{bmatrix} \quad (1)$$

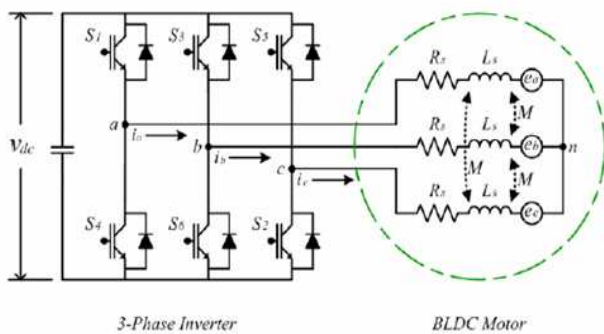


Fig. 1 Block diagram of a BLDC motor drive.

The torque equation is given by:

$$T_s = \frac{e_a \cdot i_a + e_b \cdot i_b + e_c \cdot i_c}{\omega_m} \quad (2)$$

where v_a , v_b , and v_c are phase voltages. R_s is a stator resistance. i_a , i_b , and i_c are phase currents. L_s is a stator inductance. M is a mutual inductance. L represents $L_s - M$. e_a , e_b , and e_c are phase back-EMFs. ω_m is a mechanical angular velocity. Fig. 2 shows that the torque ripple can be minimized and the stable control is achieved when the phase current with square wave form is injected into the part where the magnitude of back-EMFs is fixed.

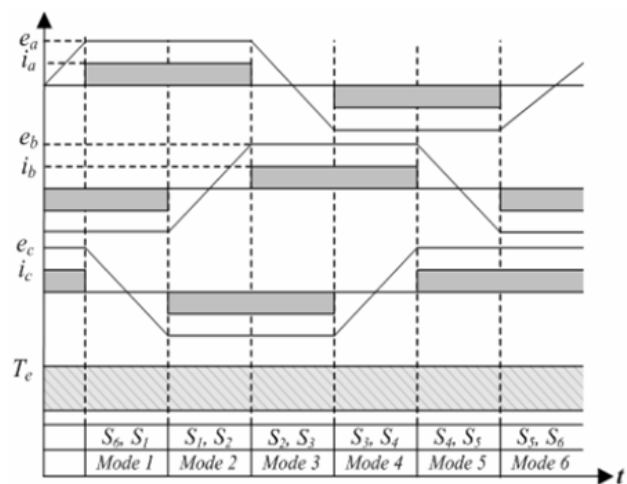


Fig. 2 Waveforms of a back-EMF, a phase current and a torque of BLDC motor.

III. PROPOSED SENSORLESS CONTROL METHOD

In the proposed sensorless control method it is possible to detect the rotor position by a trapezoidal back-EMF of BLDC motors. The back-EMF is estimated by an unknown input observer as it is not measured directly. The sensorless control method using an unknown input observer is obtained as follows:

A. The unknown input observer is considered by the following line-to-line equation:

The unknown input observer is considered by the following line-to-line equation:

$$i_{ab} = -\frac{2R_s}{2L} i_{ab} + \frac{1}{2L} v_{ab} - \frac{1}{2L} e_{ab} \quad (3)$$

In (3), i_{ab} and v_{ab} can be measured, therefore they are considered as “known” state variables. On the other hand, since e_{ab} cannot be measured, this term is considered as an “unknown” state. The equation (3) can be rewritten in the following matrix form:

$$\dot{x} = Ax + Bu + Fw \quad (4)$$

$$y = Cx \quad (5)$$

where

$$A = \left[-\frac{2R_s}{2L} \right], B = \left[\frac{1}{2L} \right], F = \left[-\frac{1}{2L} \right]$$

$$x = [i_{ab}], u = [v_{ab}], w = [e_{ab}], y = [i_{ab}], C = [1]$$

The back-EMF is regarded as an unknown disturbance (4) and it can be represented by a differential equation:

$$\dot{z} = Dz \quad (6)$$

$$w = Hz \quad (7)$$

where

$$D = \begin{bmatrix} 0_{(\delta-1) \times 1} & I_{(\delta-1)} \\ 0_{1 \times 1} & 0_{(\delta-1)} \end{bmatrix}, H = [I_1 \quad 0_{1 \times (\delta-1)}]$$

I is identity matrix, and δ is degree of polynomial expression under:

$$w = \sum_{i=0}^{\delta} a_i t^i, \delta \geq 1. \quad (8)$$

where a_i denotes a set of unknown coefficient vectors.

In (8) a_i can be defined as $a_i = 0$ if there is no experimental information about disturbance. The unknown disturbance w

is modeled by the completely observable dynamical system of (6, 7). Therefore, the entire system can be expressed by the augmented equation that introduces disturbances of differential equation form modeling the back-EMF. The augmented model can be shown as (9) and (10):

$$\dot{x}_a = A_a x_a + B_a u \quad (9)$$

$$y = C_a x_a \quad (10)$$

where

$$A_a = \begin{bmatrix} A & FH \\ 0 & E \end{bmatrix} = \begin{bmatrix} -\frac{2R_s}{2L} & -\frac{1}{2L} \\ 0 & 0 \end{bmatrix}, x_a = \begin{bmatrix} i_{ab} \\ e_{ab} \end{bmatrix},$$

$$B_a = \begin{bmatrix} B \\ 0 \end{bmatrix} = \begin{bmatrix} 1 \\ 0 \end{bmatrix}, u = [v_{ab}], y = [i_{ab}],$$

$$C_a = [C \ 0] = [1 \ 0]$$

and the degree of polynomial expression for disturbance is established by $\delta = 1$. Since systems of (9) and (10) are observable [20], it is possible to compose the following observer:

$$\dot{\hat{x}}_a = A_a \hat{x}_a + B_a u + K(y - \hat{y}) \quad (11)$$

K is the gain matrix of the observer [19]. If the gain of the observer is selected properly, this observer can accurately estimate line-to-line currents and back-EMFs of motors. Fig. 3 shows a block diagram of the proposed back-EMF observer.

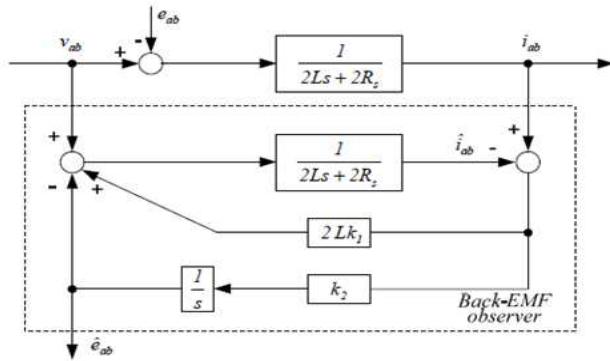


Fig. 3 Block diagram of the proposed back-EMF observer.

Therefore, the equation of whole observer including all three phases is as follows:

$$\frac{d}{dt} \begin{bmatrix} \hat{i}_{ab} \\ \hat{e}_{ab} \\ \hat{i}_{bc} \\ \hat{e}_{bc} \\ \hat{i}_{ca} \\ \hat{e}_{ca} \end{bmatrix} = \begin{bmatrix} -\frac{2R_s}{2L} & -\frac{1}{2L} & 0 & 0 & 0 & 0 \\ 0 & 0 & 0 & 0 & 0 & 0 \\ 0 & 0 & -\frac{2R_s}{2L} & -\frac{1}{2L} & 0 & 0 \\ 0 & 0 & 0 & 0 & 0 & 0 \\ 0 & 0 & 0 & 0 & -\frac{2R_s}{2L} & -\frac{1}{2L} \\ 0 & 0 & 0 & 0 & 0 & 0 \end{bmatrix} \begin{bmatrix} \hat{i}_{ab} \\ \hat{e}_{ab} \\ \hat{i}_{bc} \\ \hat{e}_{bc} \\ \hat{i}_{ca} \\ \hat{e}_{ca} \end{bmatrix} + \begin{bmatrix} \frac{1}{2L} & 0 & 0 \\ 0 & 0 & 0 \\ 0 & \frac{1}{2L} & 0 \\ 0 & 0 & 0 \\ 0 & 0 & \frac{1}{2L} \\ 0 & 0 & 0 \end{bmatrix} \begin{bmatrix} v_{ab} \\ v_{bc} \\ v_{ca} \end{bmatrix} + \begin{bmatrix} k_1 & 0 & 0 \\ k_2 & 0 & 0 \\ 0 & k_3 & 0 \\ 0 & k_4 & 0 \\ 0 & 0 & k_5 \\ 0 & 0 & k_6 \end{bmatrix} \begin{bmatrix} i_{ab} - \hat{i}_{ab} \\ i_{bc} - \hat{i}_{bc} \\ i_{ca} - \hat{i}_{ca} \end{bmatrix} \quad (12)$$

B. Estimation of Position and Speed

If the estimated magnitude of a back-EMF is defined, the

rotor position and the speed can be calculated by simple arithmetic. The relationship between the speed and the magnitude of a back-EMF in BLDC motors is:

$$E = K_e \hat{\omega}_e \quad (13)$$

where E is a back-EMF magnitude, K_e is a back-EMF constant, and $\hat{\omega}_e$ is an electrical angular velocity.

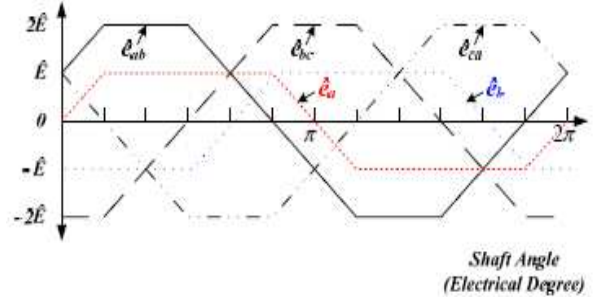


Fig. 4 Relation between estimated line-to-line back-EMFs and estimated back-EMFs.

As shown in Fig. 4, the magnitude of the back-EMF is estimated by the maximum magnitude of the line to-line back-EMF that the unknown input observer offers. Therefore, the speed can be calculated by using the estimated magnitude of the back-EMF as follows:

$$\hat{\omega}_e = \frac{E}{K_e} \quad (14)$$

$$\hat{\omega}_m = \frac{2}{P} \hat{\omega}_e \quad (15)$$

where $\hat{\omega}_m$ is an estimated mechanical angular velocity and P is the number of poles. The rotor position is obtained by integrating the motor speed:

$$\hat{\theta} = \int \hat{\omega}_e dt + \theta_0 \quad (16)$$

where θ_0 is the initial position of rotor.

C. Block diagram of proposed sensorless scheme

Fig. 5 illustrates the overall structure of the proposed sensorless drive system. The hysteresis current controller is used for each phase current control. The line-to-line voltage is calculated based on the DC-link voltage and switching status of the inverter. As described above, the back-EMF observer provides the estimated line-to-line back-EMF (12). The speed (15) and the rotor position (16) are calculated from the estimated line-to-line back-EMFs.

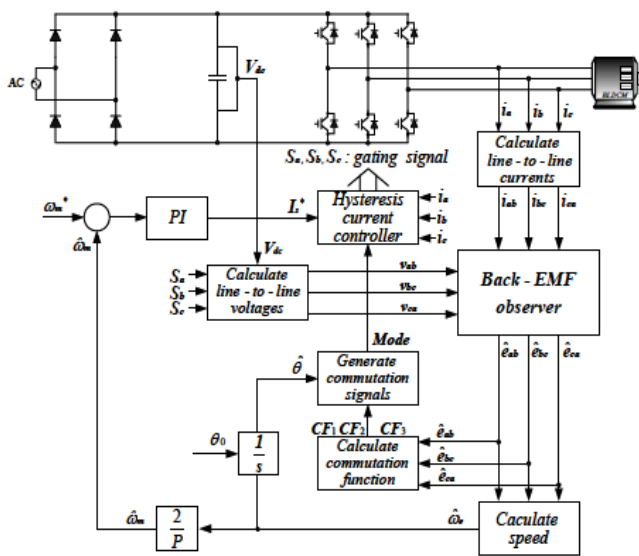


Fig. 5 Overall structure of the proposed sensorless drive system.

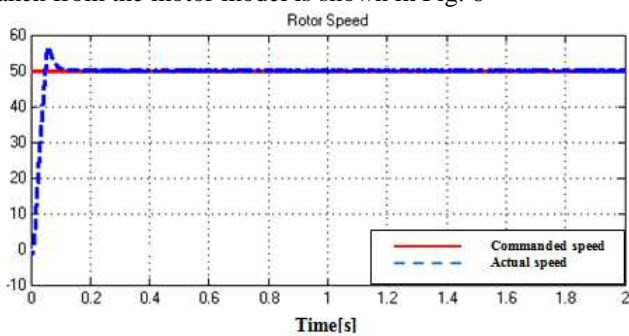
IV. SIMULATION RESULTS

Simulation is performed by Matlab/Simulink environment on the BLDC motor that has the ratings and parameters as shown in Table 1. This data corresponds to 3Hp motor [25].

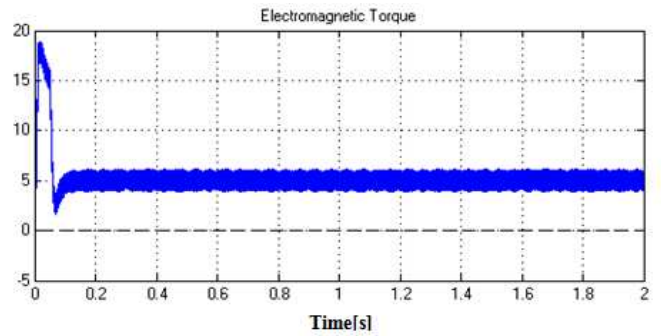
Table I. Ratings and parameters of BLDC motor.

Rated voltage	V	310(V)
Rated torque	T_e	1.5(Nm)
Rated speed	N_r	1650(rpm)
Stator resistance	R_s	0.2(Ω)
Stator inductance	L	$8.5e^{-3}$ (H)
Rotor inertia	J_m	0.089(kg.m ²)
Back-EMF constant	K_e	0.25(V/rad/sec)
No. of pole pairs	P_n	4

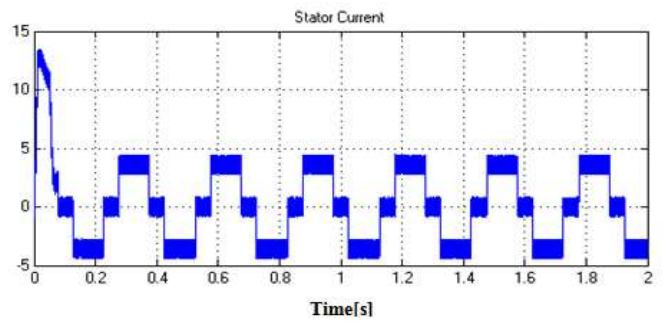
This paper evaluates the robustness of the sensorless algorithm under variations of speed reference. The actual machine speed response for the commanded speed at 50 rpm (load torque 5Nm) with speed and position feedback directly taken from the motor model is shown in Fig. 6



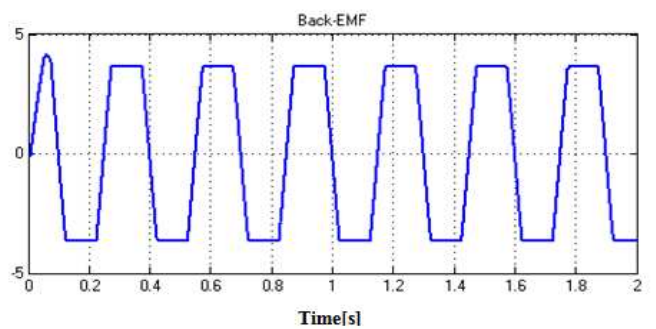
(a) Rotor Speed



(b) Electromagnetic Torque



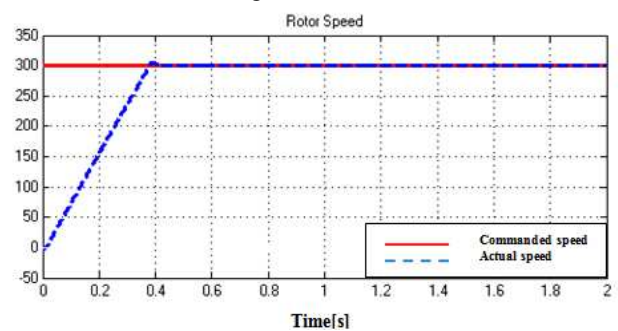
(c) Stator Current



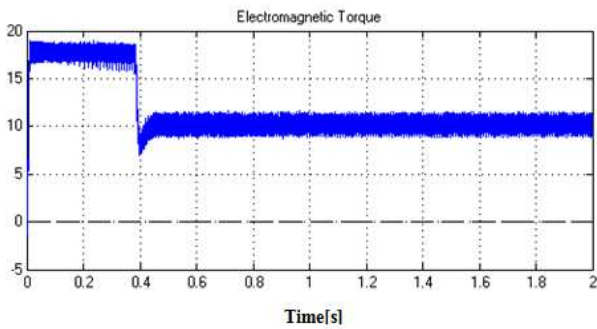
(d) Back EMF

Fig. 6 Response waveforms under step change of speed reference (50 rpm).

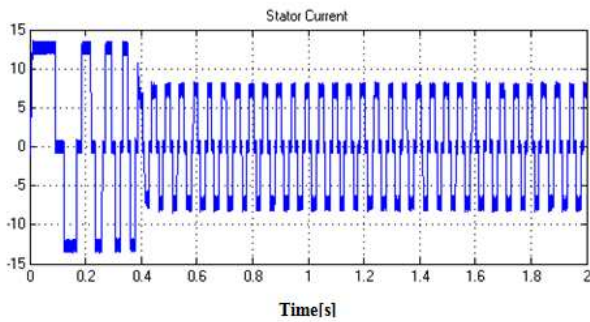
The actual machine speed response for the commanded speed at 300 rpm (load torque 10Nm) with position and speed feedback is shown in Fig.7.



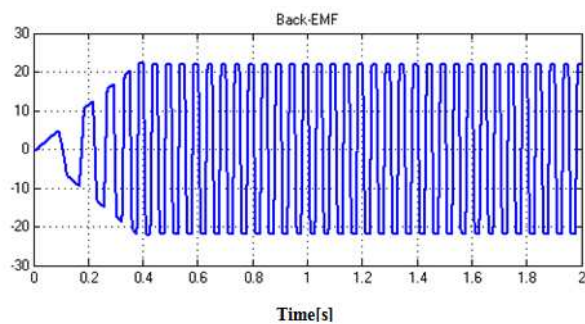
(a) Rotor Speed



(b) Electromagnetic Torque



(c) Stator Current

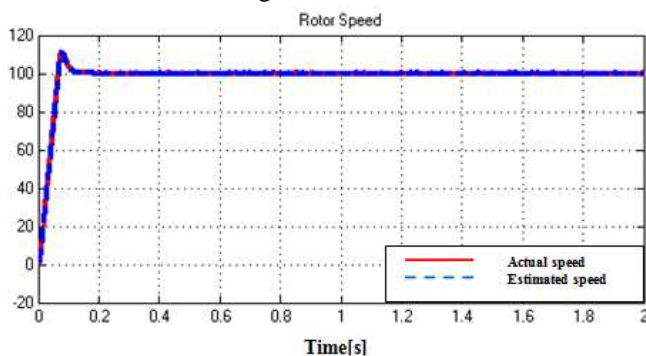


(d) Back EMF

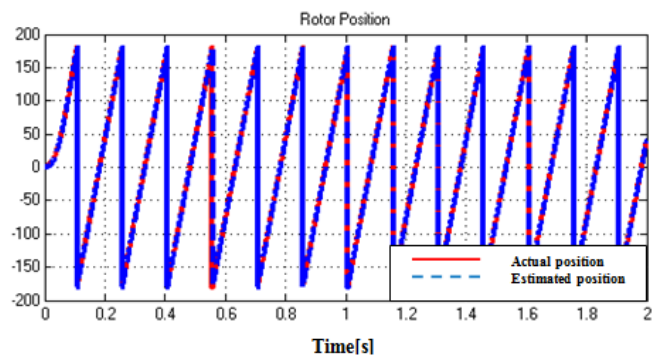
Fig. 7 Response waveforms under step change of speed reference (300 rpm).

From the Fig. 6 and 7, it is clear that the tracking of commanded speed is effective and accurate by the actual motor speed with the designed controller with no oscillations in the speed.

The actual machine speed and estimated speed response for the commanded speed at 100 rpm with speed and position feedback obtained from the back-EMF observer and corresponding estimated and actual rotor position of the machine are shown in Fig. 8.



(a) Actual and Estimated speed



(b) Actual and Estimated position

Fig. 8 Response waveforms of actual and estimated speed, rotor position under step change of speed reference (100 rpm)

From the Fig.8 it is clear that the designed back-EMF observer tracks the actual speed and rotor position accurately and estimated speed and rotor position converges with the actual motor speed and rotor position.

Response waveforms under a step change of speed reference from 50 to 800 rpm are shown in Fig. 9. Initially the motor starts with 50 rpm at time of 1sec speed is changed to 800 rpm also the motor starts with a load torque of 0 N-m initially at 1 sec a load torque of 5 Nm is applied which is shown in Fig. 10.

The speed reference is limited by a ramp in speed controller to avoid the step-type entries. The speed reference change rate follows the acceleration and deceleration ramps you define as shown in Fig. 9 and Fig. 10 in order to avoid sudden reference changes that could cause armature over-current and destabilize the system. An excessively large positive value can cause DC bus under-voltage.

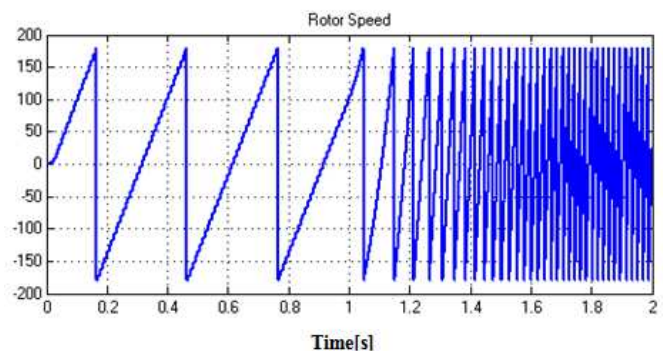
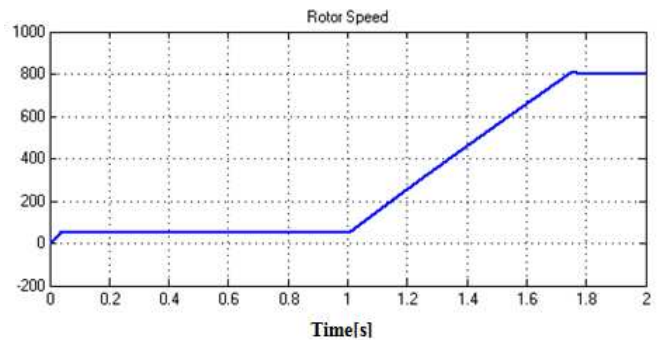


Fig. 9 Response waveforms under a step change of speed reference from 50 to 800 rpm.

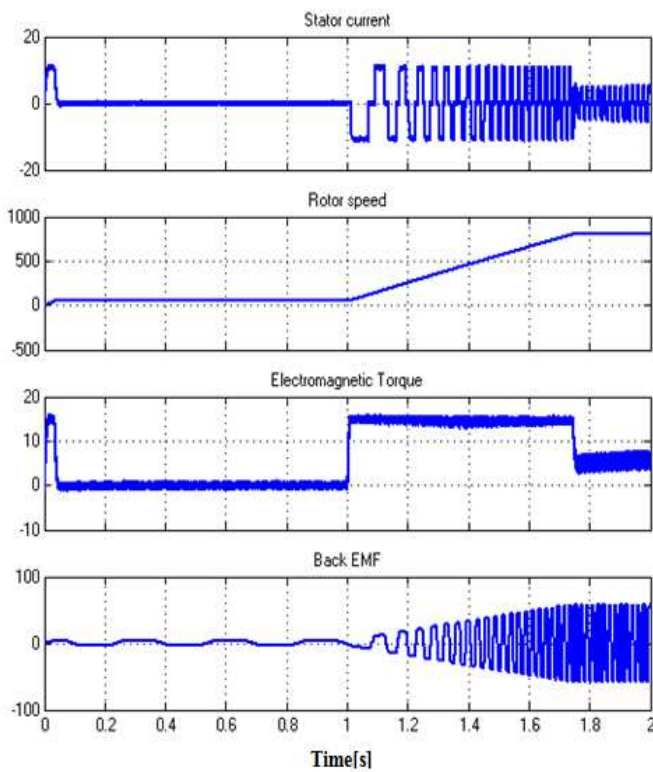


Fig. 10 BLDC motor Speed, Torque, Stator current and Back-EMF

It is clearly verified from this test that the proposed sensorless drive algorithm has good transient response under various speed operating conditions.

The back-EMF observer is designed to estimate the back-EMF. The estimated back-EMF waveforms for the speed reference change of 50 to 800 rpm are shown in Fig. 11 and also the actual stator current waveforms are shown in Fig. 12.

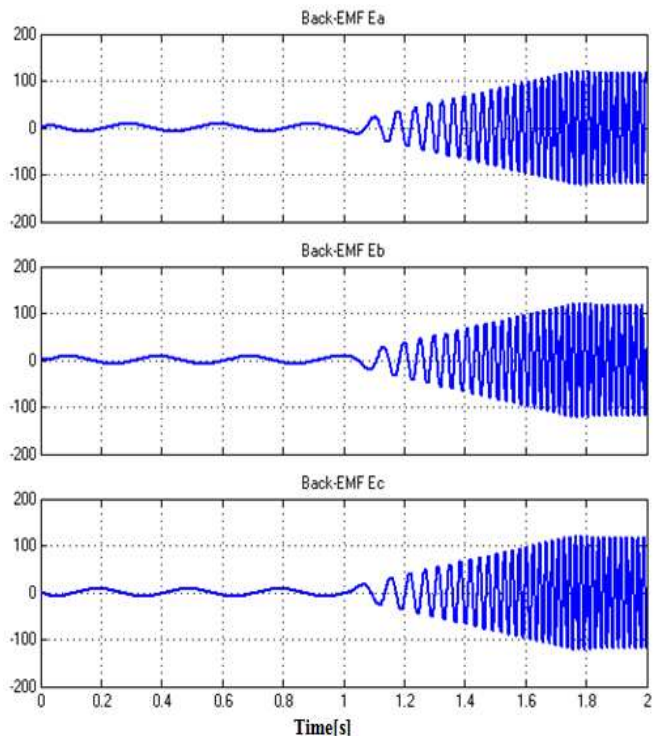


Fig. 11 Estimated Back-EMF by Back-EMF Observer

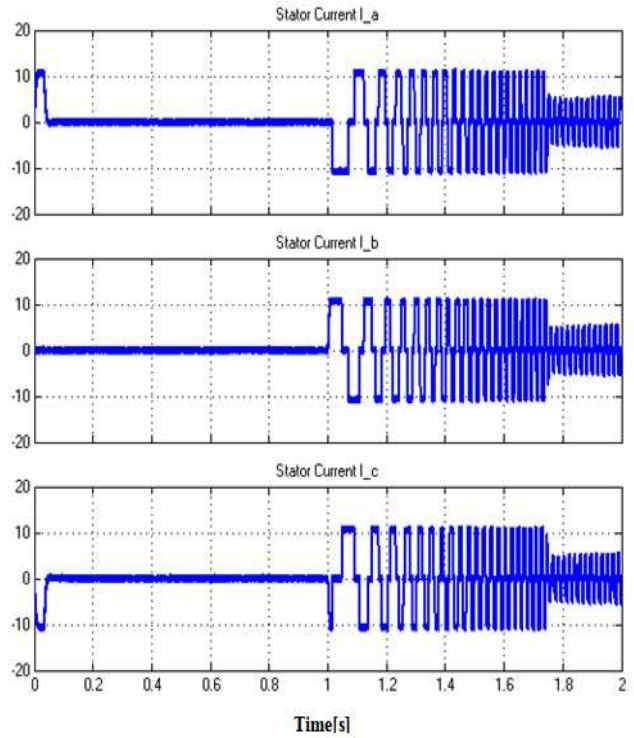


Fig. 12 BLDC motor Stator Current waveforms

V. CONCLUSION

Speed control of BLDC motor without rotor position sensors based on Back-EMF observer is presented in this paper. The equation of augmented system and an estimated line-to-line back-EMF are used in order to obtain the observer effectively. Therefore the actual rotor position and also the machine speed can be estimated from the estimated line-to-line back-EMF even in the transient state. This sensorless method using an unknown input observer can

- Be accomplished without additional circuits.
- Detect the rotor speed and position effectively over a full speed range, especially at a low speed range.
- Be easily realized for industry application by simple control algorithm.

REFERENCES

- [1] N. Matsui, "Sensorless PM brushless DC motor drives," *IEEE Trans. on Industrial Electronics*, vol. 43, no. 2, pp. 300-308, 1996.
- [2] K. Xin, Q. Zhan, and J. Luo, "A new simple sensorless control method for switched reluctance motor drives," *KIEE J. Electr. Eng. Technol.*, vol. 1, no. 1, pp. 52-57, 2006.
- [3] S. Ogasawara and H. Akagi, "An approach to position sensorless drive for brushless DC motors," *IEEE Trans. on Industry Applications*, vol. 27, no. 5, pp. 928-933, 1991.
- [4] J. C. Moreira, "Indirect sensing for rotor flux position of permanent magnet AC motors operating over a wide speed range," *IEEE Trans. on Industry Applications*, vol. 32, no. 6, pp. 1394-1401, 1996.
- [5] J. X. Shen, Z. Q. Zhu, and D. Howe, "Sensorless flux-weakening control of permanent-magnet brushless machines using third harmonic back EMF," *IEEE Trans. on Industry Applications*, vol. 40, no. 6, pp. 1629-1636, 2004.
- [6] T. M. Jahns, R. C. Becerra, and M. Ehsani, "Integrated current regulation for a brushless ECM drive," *IEEE Trans. on Power Electronics*, vol. 6, no. 1, pp. 118-126, 1991.

- [7] H. R. Andersen and J. K. Pedersen, "Sensorless ELBERFELD control of brushless DC motors for energy-optimized variable-speed household refrigerators," *EPE Conf. Rec.*, vol. 1, pp. 314-318, 1997.
- [8] G. J. Su and J. W. Mckeever, "Low cost sensorless control of brushless DC motors with improved speed range," *IEEE Trans. on Power Electronics*, vol. 19, pp. 296-302, 2004.
- [9] K. Iizuka, H. Uzuhashi, and M. Kano, "Microcomputer control for sensorless brushless motor," *IEEE Trans. on Industry Applications*, vol. 27, pp. 595-601, 1985.
- [10] H. G. Yee, C. S. Hong, J. Y. Yoo, H. G. Jang, Y. D. Bae, and Y. S. Park, "Sensorless drive for interior permanent magnet brushless DC motors," *Proc. of IEEE International Conf. on Electric Machines and Drives*, 18-21, pp. TD1/3.1-3.3, 1997.
- [11] Q. Jiang, C. Bi, and R. Huang, "A new phaselay-free method to detect back EMF zero-crossing points for sensorless control of spindle motors," *IEEE Trans. Magn.*, vol. 41, no. 7, pp. 2287-2294, 2005.
- [12] A. T. Alexandridis and G. D. Galanos, "Design of an optimal current regulator for weak AC/DC systems using Kalman filtering in the presence of unknown inputs," *Proc. IEE*, vol. 136, no. 2, pp. 57-63, 1989.
- [13] M. Saif, "Robust servo design with applications," *Proc. Inst. Elect. Eng.*, vol. 140, no. 2, pp. 87-92, 1993.
- [14] M. Aldeen and J. F. Marsh, "Decentralised observer-based control scheme for interconnected dynamical systems with unknown inputs," *Proc. Inst. Elect. Eng.*, vol. 146, no. 5, pp. 349-358, 1999.
- [15] T. G. Park, J. S. Ryu, and K. S. Lee, "Actuator fault estimation with disturbance decoupling," *Proc. Inst. Elect. Eng.*, vol. 147, no. 5, pp. 501-508, 2000.
- [16] T. G. Park and K. S. Lee, "Process fault isolation for linear systems with unknown inputs," *Proc. Inst. Elect. Eng.*, vol. 151, no. 6, pp. 720-726, 2004.
- [17] B. Marx, D. Koenig, and J. Ragot, "Design of observers for Takagi-Sugeno descriptor systems with unknown inputs and application to fault diagnosis," *Proc. Inst. Elect. Tech.*, vol. 1, no. 5, pp. 1487-1495, 2007.
- [18] P. Pillay and R. Krishnan, "Modeling, simulation, and analysis of permanent-magnet motor drives, part II: The brushless DC motor drive," *IEEE Trans. on Industry Applications*, vol. 25, no. 2, pp. 274-279, 1989.
- [19] S. H. Huh, S. J. Seo, I. Choy, and G. T. Park, "Design of a robust stable flux observer for induction motors," *KIEE J. Electr. Eng. Technol.*, vol. 2, no. 2, pp. 280-285, 2007.
- [20] Thoralf A. Schwarz, "Uncertainty Analysis of a Fault Detection and Isolation Scheme for Multi-Agent Systems", Master's thesis, KTH, Sweden, 2012.
- [21] C. L. Baratieri and H. Pinheiro, "Sensorless Vector Control for PM Brushless Motors with Nonsinusoidal Back-EMF", *IEEE International Conference on Electrical Machines*, 2014, 915-921
- [22] P. Lei, W. Bei-Bei and S. He-Xu, "A Novel Control Method for BLDCM Based on Phase Back-EMF Observation", *Research Journal of Applied Sciences, Engineering and Technology*, 6(13), 2013, 2474-2482.
- [23] S. Wang, C. Lu, and A. Lee, "Disturbance Observer Structure Applied to Sensorless Brushless DC Motors Drive", *International Journal of Computer Theory and Engineering*, 7(2), 2015, 92-96
- [24] Bahram Shafai, "Proportional integral observer in robust control, fault detection and decentralized control of dynamic systems", To appear in book 21 (2015), 1087-1091.
- [25] Boss Brushless DC motor, BOSS04 (115 or 230VAC), Manufacturing division, 901, East Thompson Avenue, Glendale, CA, 91201-2011, www.minarikcorp.com.